

The *In Vivo* Elastic Properties of the Plantar Fascia During the Contact Phase of Walking

Amit Gefen
Tel Aviv, Israel

ABSTRACT

The *in vivo* elastic properties of the plantar fascia during the contact phase of walking were determined experimentally by integrating a pressure-sensitive optical gait platform with a radiographic fluoroscopy system for recording skeletal motion. In order to calculate the fascia's tension-deformation relation, lateral images of the foot's skeleton that allowed evaluation of the fascia's transient length from the arch-contact to toe-off stages of walking were obtained simultaneously with the vertical foot-ground contact forces. The plantar fascia was shown to undergo continuous elongation from arch-contact to toe-off, reaching a deformation of 9 to 12% between these positions. Rapid elongation of the fascia, at a strain rate of about 0.9 ± 0.1 Sec⁻¹, was observed before and immediately after mid-stance, while a significantly slower elongation occurred at a strain rate of approximately 0.2 ± 0.1 Sec⁻¹ around push-off and toe-off. The average stiffness of the fascia at the slow-to-moderate walking velocities was 170 ± 45 N/mm, which is similar to reported stiffness values for cadaver fascia specimens. The present technique may be useful for validation of computational models of the soft tissues of the foot as well as for testing the effectiveness of orthoses and shoe types for relieving excessive strain of the fascia in the treatment of plantar fasciitis.

Key Words: Foot; Gait; Soft Tissue Mechanical Properties; Foot-ground Pressure; Fluoroscopy.

INTRODUCTION

During load bearing, the plantar fascia functions to support the foot's arch and absorb some of the foot-ground

impact energy through deformation.¹⁻³ Abnormal foot structures, such as those characterized by an excessively high arch, may overload the plantar fascia and thereby lead to plantar fasciitis, an inflammatory and painful condition that results from micro tears in the fascia.⁴ When pharmaceutical treatment of plantar fasciitis fails, surgical release of the fascia may be performed to partially or fully detach it from the calcaneal tuberosity.⁵ Effective treatment of this clinical condition requires quantitative information on the normal, tolerable deformations and strains of the plantar fascia during actual walking, and these are not yet clear.

The plantar fascia is subjected to significant traction as body weight is transferred onto the forefoot during the latter half of the contact phase of walking, and the intensity of the fascia's stresses and strains increases with the intensity of activity.⁶ Although several measurements of strain in the plantar fascia of cadaver feet have been reported,⁷⁻¹¹ they were by definition *in vitro* setups in which musculoskeletal loading of the foot was simulated using instrumented mechanical apparatuses. The present paper describes a technique that allows direct measurements of the *in vivo* deformations and strains of the plantar fascia during the latter half of the contact phase of gait. It also enables the evaluation of the internal tension forces that are being carried by the fascia at this stage, which can, in turn, be correlated with the measured elongation to calculate the fascia's *in vivo* stiffness. Hence, the present analysis provides insight into the functional role of the plantar fascia in stabilizing the foot's arch and in dissipating energy through deformation.

METHODS

Two quantifying methods were integrated to simultaneously record the deformation of the plantar fascia and the vertical forces developing during the foot-ground contact. A digital radiographic fluoroscopy (DRF) imaging system was used to measure the transient distance between the insertion surfaces of the plantar fascia as seen from the lateral view, while the measurements carried out by a dynamic foot-ground

Corresponding Author:
Dr. Amit Gefen
Department of Biomedical Engineering, Faculty of Engineering
Tel Aviv University
Tel Aviv 69978 Israel
Phone: +972-3-640-8093
Fax: +972-3-640-5845
E-mail: gefen@eng.tau.ac.il

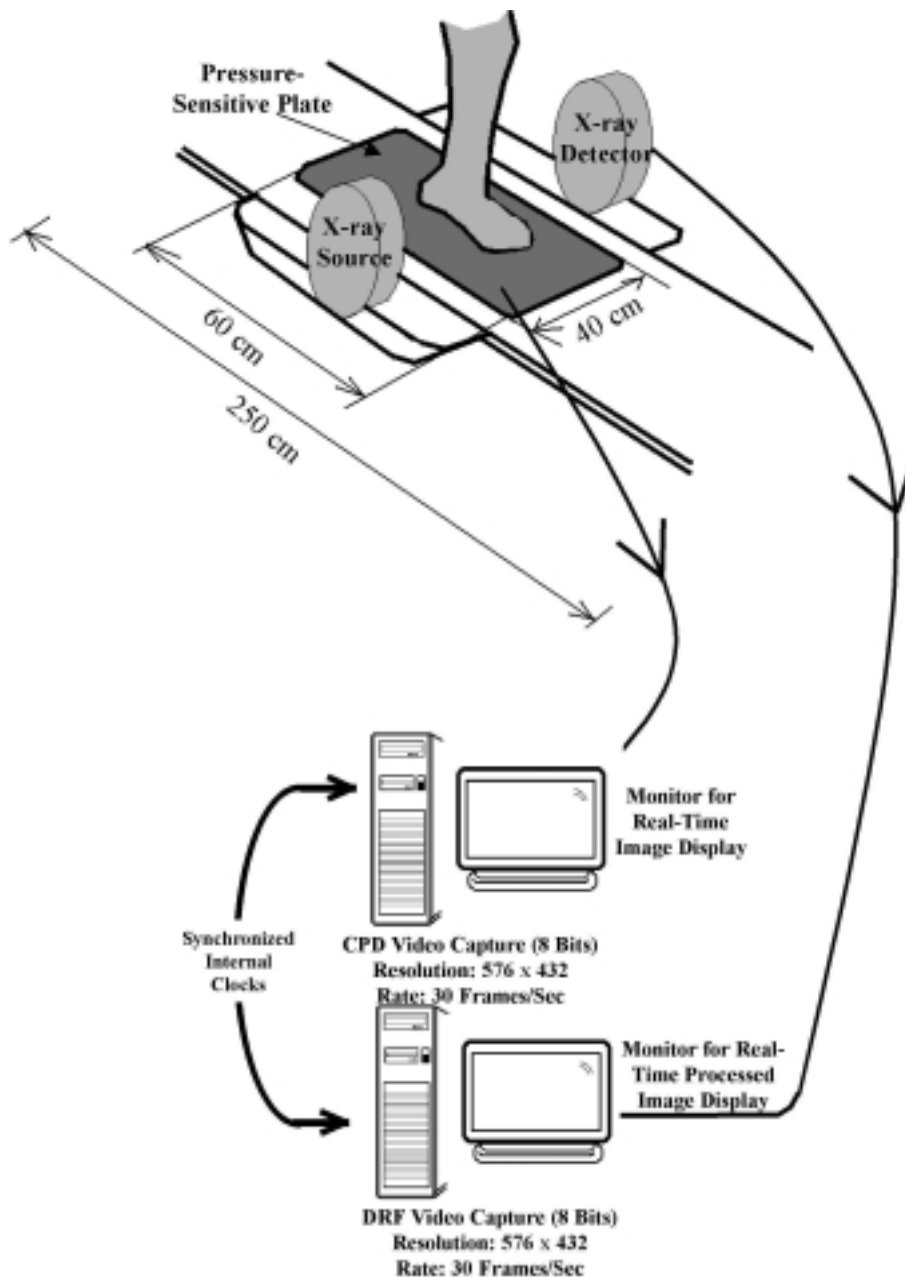


Fig. 1: A schematic drawing of the DRF/CPD experimental arrangement. The pressure-sensitive contact pressure display (CPD) plate is embedded within the digital radiographic fluoroscopy (DRF) system and is placed between the source and detector of the X-ray radiation. This allows simultaneous measurements of the plantar pressure evolution with the foot's skeletal motion during the contact phase of walking.

contact pressure display (CPD) provided the reading of ground reactions under the foot (Fig. 1). The Philips Multi Diagnost 3 (MD3) DRF system was used for the radiographic measurements. The optical CPD method¹²⁻¹⁵ was selected for recording plantar pressures because of its versatility in providing the means for constructing a pressure-sensitive area in dimensions that could be easily fitted into the DRF system.

Digital sampling of the CPD images was carried out using a 1/2" CCD video camera with 600 TV lines (Chiper, CPT-8360).

A DRF/CPD gait platform with a length of 2.5 m was mounted on the MD3 examination table. The subjects were hand-supported while they walked for a feeling of greater safety. This was considered during the measurements by training subjects prior to data acquisition to avoid transferring weight to the rails of the gait platform. Using a digital video capture board (Miro 20TD), the initial sampling rate of DRF/CPD frames was determined to be 80 Hz and, after the distorted frames were removed, a set of up to 30 per Sec high-quality frames with a resolution of 576 x 432 pixels was obtained for each completed contact phase of walking. Two female volunteers with similar body characteristics (27 and 35 years of age and weighing 58 and 60 Kg) were protected by wearing a lead apron (4 Kg) to minimize exposure to X-ray radiation and limit it to the feet. Each subject carried out four trials of walking on the DRF/CPD gait platform. Their gait velocity ranged between 0.5 to 0.9 m/Sec. The DRF/CPD data were analyzed using video and image processing software to obtain the time-dependent deformation of the plantar fascia with respect to the foot-ground vertical contact forces. Using an image processing software package, the length of the plantar fascia was digitally measured from two well-defined points on each of the DRF frames obtained from the arch-contact to the toe-off stages of the stance phase. These points were the tubercle on the plantar surface of the calcaneus proximally and the most distal point on the convexity of the head of the first metatarsal distally.

The plantar fascia was assumed to be in a position of its neutral length when the foot's arch was in a very early stage of contact with the ground ("arch-contact," Fig. 2a), before the arch was flattened under body weight and before any forefoot contact was made. The DRF frame that most closely captured this position was

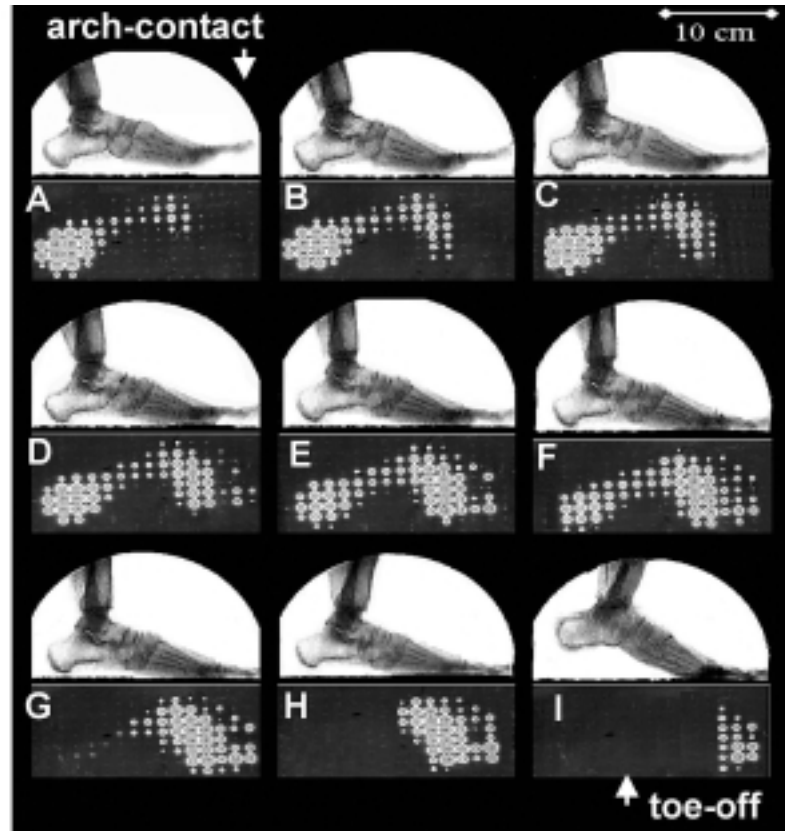
located by scanning the progression of the simultaneously captured CPD plantar pressure distributions in search for the ones showing early arch contact (Fig. 2a). Consequently, the angle of the foot's arch (formed between the talus apex, calcaneus plantar surface and metatarsal heads) was measured for the selected and near frames, in order to ensure that the one chosen for measuring the neutral fascia's length was captured just before the arch had become flattened by full weight bearing. The fascia's length was monitored from this point to the toe-off stage, and representative findings are plotted in Figure 2b. An error of 0.2 mm in the length measurements that was due to the spatial resolution of the acquired digital images was accounted for. The value of the absolute plantar fascia's deformation was calculated for each DRF frame following arch-contact as being the difference between the loaded and neutral lengths of the fascia. The tensile strain of the fascia was calculated as the ratio of absolute deformation to the above neutral fascia's length.

Two geometric measurements were taken digitally on each DRF frame:

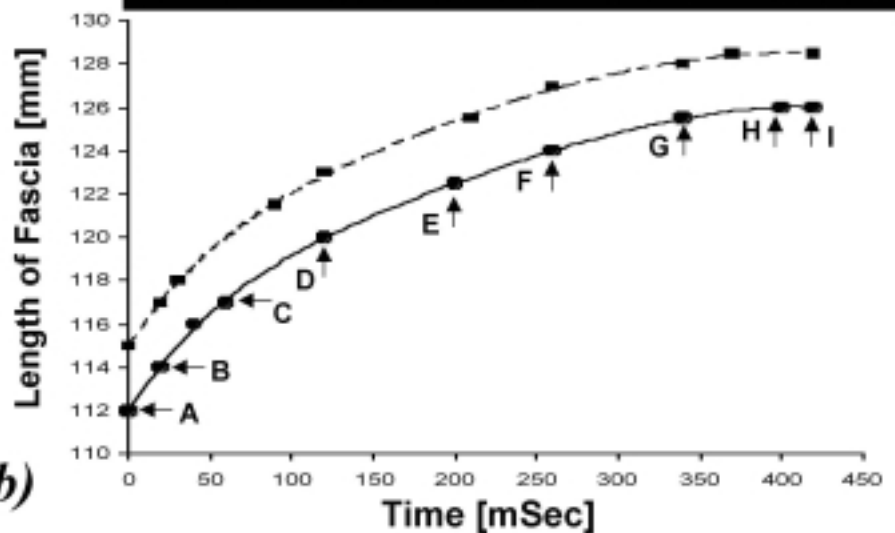
- (i) the horizontal projection of the forefoot's length and
- (ii) the arch's height.

This was done to interpret the vertical ground reaction forces measured by CPD in terms of the tension resulting in the plantar fascia while both the hindfoot and forefoot are being supported (from arch-contact to heel-rise). These dimensions were subsequently used for balance of forces and moments in the foot's structure, assuming that as the arch loses height, the foot lengthens through a hinge-type mechanism based at the apex of the arch (Fig. 3).

Intrinsic muscle activity at the sole of the foot as well as extrinsic muscle activity along the anterior and posterior tibia may affect the rigidity of the arch.



(a)



(b)

Fig. 2: (a) Representative DRF/CPD data of a single stance phase of barefoot walking, from arch-contact to toe-off. (b) Typical elongation of the plantar fascia with time during the latter stage of the stance phase for the two subjects marked as I (solid line) and II (dashed line). The DRF/CPD images (A through I) that correspond to the data points of subject I are shown in Fig. 2a. DRF= digital radiographic fluoroscopy; CPD= contact pressure display.

However, quantitative evaluations of intrinsic or extrinsic muscle forces *in vivo* are difficult to obtain and require many assumptions concerning the musculoskeletal structures and their biomechanical function. For the purpose of calculating tension in the plantar fascia, and in

lack of quantitative information about subject-specific extrinsic and intrinsic muscle forces produced during midstance, the foot was modeled herein as a passive mechanism (Fig. 3), and this should be taken into account while interpreting the results.

Given the above assumptions, it was concluded that the amount of tension in the plantar fascia that existed while the hindfoot and forefoot were concurrently supported could be approximated as being dependent upon three variables:

- (i) the vertical reaction force (in Newtons) under the forefoot (F_f), calculated by summation of CPD contact force readings under the forefoot-ground contact region (Fig. 2a);
- (ii) the horizontal projection of the forefoot's length (l_1), and
- (iii) the arch's height (l_2).⁷

The magnitude of each of these three variables alters with the evolution of the contact phase, and all three are measured simultaneously using the integrated DRF/CPD apparatus, which allows the evaluation of the build-up of tension in the fascia as a function of its elongation. It should be noted that this simple quasi-steady modeling of the foot's structure for calculating the tension in the fascia is only valid while both the heel and the forefoot are in some contact with the ground and, accordingly, only the DRF/CPD frames that clearly showed such contact under both the heel and forefoot (from arch-contact to heel-rise) were used for this analysis.

RESULTS

High-quality lateral DRF images were consistently obtained using the integrative DRF/CPD gait platform and digital recording system. Representative elongation-versus-time curves for the plantar fascia during the contact phase of walking, from arch-contact to toe-off, are plotted in Fig. 2b. The neutral length, the maximal absolute deformation (calculated as the maximal difference between the loaded and neutral lengths) and the maximal strain of the plantar fascia (calculated as the ratio of absolute maximal deformation to the neutral length) were obtained for the two subjects, and are specified in Table 1. The fascia was shown to undergo continuous elongation from arch-contact to toe-off, reaching a deformation of 9% to

12% between these positions. Before and immediately after midstance, the plantar fascia was shown to elongate rapidly, at a strain rate of about $0.9 \pm 0.1 \text{ Sec}^{-1}$, to accommodate for the weight-bearing position. Contrarily, significantly slower elongation was observed toward push-off and until the end of the contact phase, at a strain rate of about $0.2 \pm 0.1 \text{ Sec}^{-1}$. The elongation versus time curves could be consistently fitted to a third-order polynomial relation of the type

$$\delta = at^3 + bt^2 + ct + d_0$$

with correlation coefficients in the range of 0.98 to 0.99, where t is the time measured (in mSec) from the

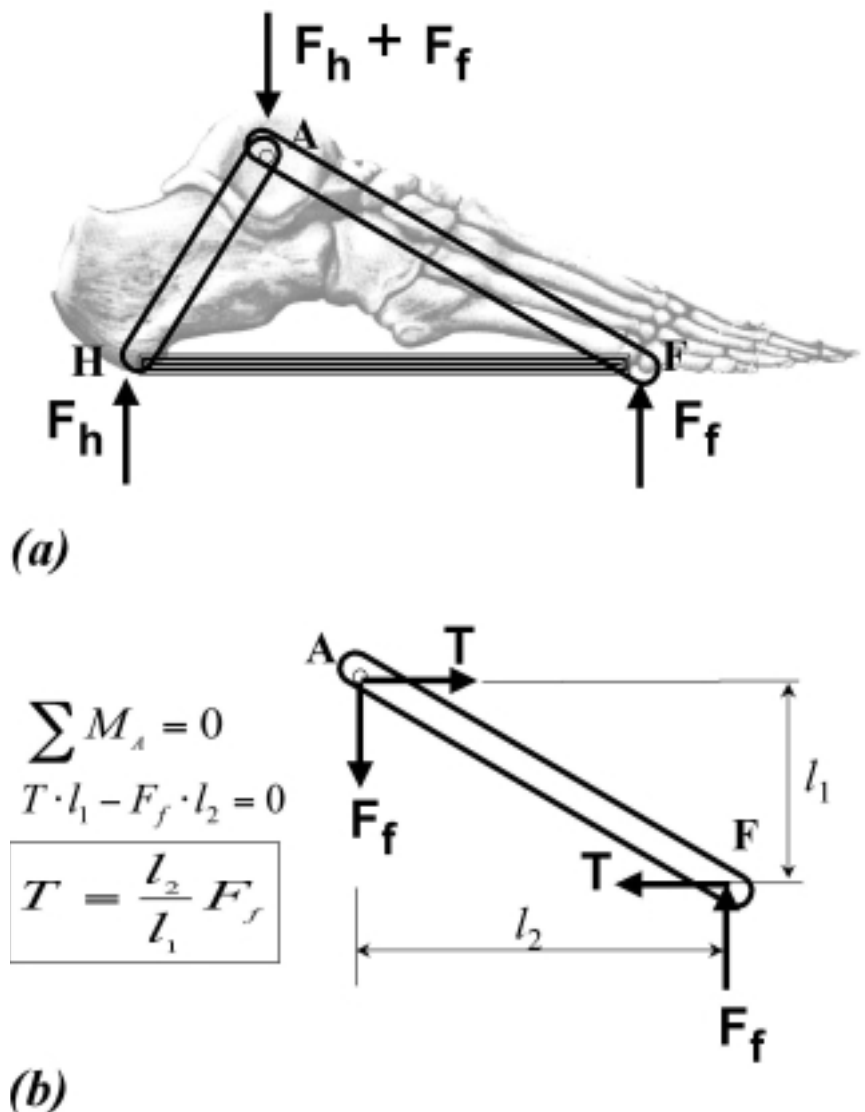


Fig. 3: Calculation of tension in the plantar fascia from arch-contact to heel-rise: **(a)** the foot is modeled as a truss subjected, at its apex, to the body's weight ($F_h + F_f$) which is balanced by the vertical ground reaction forces at the hindfoot (F_h) and forefoot (F_f). **(b)** Balance of moments ($\sum M_A = 0$) is carried out around the ankle joint (point A) in a "free-body-diagram" of the forefoot element, to evaluate the resulting tension in the fascia (T). The tension in the fascia is shown to be dependent upon the forefoot-ground reaction force (F_f), the height of the arch (l_1) and the horizontal projection of the forefoot's length (l_2).

event of arch-contact for reaching a length δ of the fascia (in mm), and a_0 to a_3 are constants.

The tension force in the plantar fascia (T) was calculated for each DRF/CPD frame that had been obtained from the arch-contact to the heel-rise stages by substituting the respectively measured forefoot-ground vertical reaction (F_f), arch height (l_i) and horizontal projection of the forefoot's length (l_2) in the relation $T=(l_2/l_i) \cdot F_f$ developed according to the moment balance in Figure 3. The calculated tension was plotted against the corresponding elongation of the fascia in order to obtain the *in vivo* elastic behavior and stiffness during the stance phase of walking in the slow-to-moderate velocities, and typical results are shown in Figure 4. The mean stiffness that had resulted by calculating the initial slopes of the tension-elongation curves obtained for all eight tests was found to be 170 ± 45 N/mm. The stiffness values found for each subject are detailed in Table 1. The elastic energy stored in the fascia from arch-contact to heel-rise (which equals the area bounded under the force-elongation curves of Fig. 4) was found to range between 6.5 and 7.9 Joule.

DISCUSSION

A technique (DRF/CPD) for measuring the plantar fascia's elongation in the latter stages of the contact phase of walking simultaneously with the vertical ground forces applied to the foot is presented. It allows *in vivo* evaluation of the force-elongation relationship for the plantar fascia, and appears to be applicable for use in the clinical setting, where it can be integrated into examinations of the foot and gait performances. In particular, this method is potentially useful for patients who demonstrate symptoms of plantar fasciitis for whom the effects of different therapeutic orthoses or footwear aimed to relieve the excessive strain may be evaluated, both pre- and post-treatment.

The strength of the present technique lies in the simultaneous measurements of the vertical ground reactions under the foot and the fascia's deformation for which the optical CPD plate is embedded within a conventional clinical fluoroscopic imaging system. It should be noted, however, that the one-dimensional approach of measuring the deformation of the plantar fascia using lateral X-ray projections place some limitations on the

Table 1: Body characteristics of subjects, and the mean \pm SD of lengths, strains and stiffness values for their plantar fascia.

		Subject I	Subject II
Age	[Years]	27	35
Weight	[Kg]	58	60
Fascia's Length at Arch-Contact	[mm]	112 ± 1.5	115 ± 1.5
Fascia's Length at Toe-Off	[mm]	125 ± 2.0	128 ± 1.5
Maximal Deformation	[mm]	13 ± 2.0	13 ± 1.5
Maximal Strain	[%]	11.6 ± 1.8	11.3 ± 1.3
Average Stiffness of Fascia	[N/mm]	112 ± 7	225 ± 9

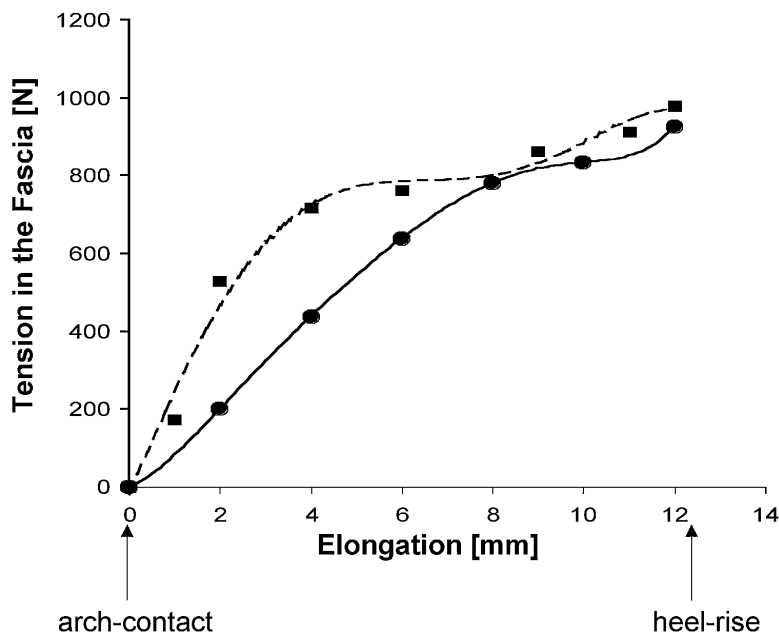


Fig. 4: Representative relations of elongation of the plantar fascia with the tensile force it is carrying from the arch-contact to the heel-rise stages of the contact phase of walking, for the two subjects represented by a solid and a dashed line.

interpretation of the results, since the true nature of the fascia's deformation is, of course, three-dimensional. The necessity to add a 4 Kg lead apron to the subject's weight was likely to further affect the measurements. In addition, the limitations of the physical structure of a DRF system designed for the clinical setting prevented the construction of a longer gait platform for measurements of the plantar fascia's properties at higher gait velocities. The model used to evaluate tension in the fascia (Fig. 3) is a simple one and does not account for tension in underlying ligamentous structures (e.g., the long plantar ligaments) that may share the traction when the fascia is elongated. However, since the fascia is considered the main restraining element that supports the arch,^{3,16} ignoring the contribution of those ligaments could be justified for the purpose of modeling.

It was demonstrated that the fascia elongates more rapidly during weight acceptance and midstance of the contact phase of barefoot walking. A slower elongation during push-off and toe-off follows the initially rapid deformation. This behavior may be explained by the histological appearance of the plantar fascia, which is composed of both collagen and elastic fibers. The elastic fibers show considerable difference in thickness and are arranged predominantly in strands and bundle-like networks in the abundant interstitial tissue.² During the contact phase of walking, both the collagen and elastic fibers change from a wavy to a straight configuration as stress is applied. Having a lower modulus of elasticity compared to collagen, the elastic fibers contribute their structural support in early extension of the fascia (around midstance), while the stretching of collagen produces restraining effects on the elongation occurring at the late extension phase (toward push-off and toe-off).

In the present study, the elastic stiffness of the plantar fascia during gait *in vivo* was measured to be at about 170 ± 45 N/mm. This result resembles the stiffness of intact cadaver fascia specimens, measured by Kitaoka et al.⁸ to be around 204 ± 50 N/mm, using a material testing machine and video tracking system for controlled loading and displacement monitoring, respectively. The discrepancy of about 20% between Kitaoka et al's data and the present result for the fascia's stiffness can be explained by the increase of the elastic modulus of the fascia (seen in other biological tissues as well) after more than one hour post mortem, as first observed by Smith in the early 50's.¹⁷ The *in vivo* fascia demonstrated increased stiffness at the early stages of weight acceptance (Fig. 4), and this may reflect the action of the intrinsic muscles of the foot which contract to increase the arch's stability for dynamic load-bearing. Considering the limitations of our *in vivo* DRF/CPD experiments, it was not possible to produce stress-strain comparisons since the geometrical dimensions of the fascia structures we tested are unknown. Based on the anatomical measurements of Simkin, who estimated the normal fascia's thickness as being 2 mm in average,¹⁸ however, it is possible to evaluate the tensile elastic modulus of the plantar fascia as being around 85 MPa (which equals the measured stiffness divided by the thickness). This estimation for the *in vivo* elastic modulus is again lower than the elastic moduli for cadaver fascia specimens that were measured to be around 345 MPa.¹⁷

Information on the material properties of cadaver fascia specimens is limited, and the author is not aware of any published reports on the tension-elongation relations for *in vivo* fascia. This information is essential in order to develop more accurate biomechanical models of the foot and, in particular, for validation of numerical (finite element) models of the stress-deformation

behavior of the foot during walking.¹² The expected implications for utilizing the present data in biomechanical models of the foot are in acquiring basic understanding of foot function and arch stability as well as of some related pathological conditions such as plantar fasciitis, plantar fibromatosis, and cavus (high arch) foot deformities. These conditions may be analyzed by the present technique which could provide valuable information, especially in view of the findings that surgical sectioning of the fascia to treat chronic inflammation may lead to undesirable flattening of the arch.⁸

ACKNOWLEDGMENT

Prof. Y. Itzchak and Dr. M. Megido-Ravid from the Diagnostic Imaging department of Sheba Medical Center, Israel, are thanked for assigning the fluoroscopic system for the measurements. Mr. Arie Moskovitch from Sheba is thanked for his technical assistance in obtaining the foot images. This study was supported by the Ela Kodesz Institute for Medical Engineering & Physical Sciences.

REFERENCES

1. **Snow, SW; Bohne, WH; DiCarlo, E; Chang, VK:** Anatomy of the Achilles tendon and plantar fascia in relation to the calcaneus in various age groups. *Foot Ankle Int*, **16**:418-421, 1995.
2. **Bojsen-Moller, F; Flagstad, KE:** Plantar aponeurosis and internal architecture of the ball of the foot. *J Anat*, **121**:599-611, 1976.
3. **Ker, RF; Bennet, MB; Bibby, SR; Kester, RC; Alexander, RM:** The spring in the arch of the human foot. *Nature*, **325**:147-149, 1987.
4. **Kim, W; Voloshin, AS:** Role of the plantar fascia in the load bearing capacity of the human foot. *J Biomech*, **28**:1025-1033, 1995.
5. **Sharkey, NA; Ferris, L; Donahue, SW:** Biomechanical consequences of plantar fascial release or rupture during gait: part I – disruptions in longitudinal arch conformation. *Foot Ankle Int*, **19**:812-820, 1998.
6. **Perry, J:** Anatomy and biomechanics of the hindfoot. *Clin. Orthop*, **177**:9-15, 1983.
7. **Wright, DG; Rennels, DC:** A study of the elastic properties of the plantar fascia. *J Bone Joint Surg*, **46A**:482-492, 1964.
8. **Kitaoka, HB; Luo, ZP; Growney, ES; Berglund, LJ; An, KN:** Material properties of the plantar aponeurosis. *Foot Ankle Int*, **15**:557-560, 1994.
9. **Kogler, GF; Solomonidis, SE; Paul, JP:** Biomechanics of longitudinal arch support mechanisms in foot orthoses and their effect on plantar aponeurosis strain. *Clin Biomech*, **11**:243-252, 1996.
10. **Sharkey, NA; Ferris, L; Donahue, SW:** Biomechanical consequences of plantar fascial release or rupture during gait: part I – disruptions in longitudinal arch conformation. *Foot Ankle Int*, **19**:812-820, 1998.
11. **Kogler, GF; Veer, FB; Verhulst, SJ; Solomonidis, SE; Paul, JP:** The effect of heel elevation on strain within the plantar aponeurosis: *in vitro* study. *Foot Ankle Int*, **22**:433-439, 2001.
12. **Gefen, A; Megido-Ravid, M; Itzchak, Y; Arcan, M:** Biomechanical analysis of the three-dimensional foot structure during gait – a basic tool for clinical applications. *J Biomech Eng*, **122**:630-639, 2000.
13. **Gefen, A; Megido-Ravid, M; Itzchak, Y:** *In vivo* biomechanical behavior of the human heel pad during the stance phase of gait. *J*

- Biomech, **34**:1661-1665, 2001.
14. **Gefen, A; Megido-Ravid, M; Azariah, M; Itzhak, Y; Arcan, M:** Integration of plantar soft tissue stiffness measurements in routine MRI of the diabetic foot. Clin Biomech, **16**:921-925, 2001.
 15. **Gefen, A; Megido-Ravid, M; Itzhak, Y; Arcan, M:** Analysis of muscular fatigue and foot stability during high-heeled gait. Gait Posture, **15**:56-63, 2002.
 16. **Simkin, A; Liechter, I:** Role of calcaneal inclination in the energy storage capacity of the human foot – a biomechanical model. Med Biol Eng Comput, **28**:149-152, 1990.
 17. **Smith, JW:** Elastic properties of the anterior cruciate ligament of the rabbit. J Anat, **88**:369-380, 1954.
 18. **Simkin, A:** Structural analysis of the human foot in standing posture. Ph.D. Thesis, Tel Aviv University, 1982.